Accelerated Degradation Of Copper Cold Plates In Direct-to-Chip Liquid Cooling in Data Centers

BY LOCHAN SAI REDDY CHINTHAPARTHY; SATYAM SAINI, PH.D.; PARDEEP SHAHI, PH.D.; PRATIK VITHOBA BANSODE, PH.D.; HIMANSHU GIRISHCHANDRA MODI; DEREJE AGONAFER, PH.D., ASSOCIATE MEMBER ASHRAF

Increasing demands for cloud-based computing and storage, the Internet of Things and machine learning-based applications have necessitated the use of more efficient cooling technologies. Direct-to-chip liquid cooling using cold plates has proven to be one of the most effective methods to dissipate the high heat fluxes of modern high-power CPUs and graphics processing units (GPU). While the published literature has well-documented research on the thermal aspects of direct liquid cooling, a detailed account of reliability degradation is missing. The present investigation provides an in-depth experimental analysis of the accelerated degradation of copper cold plates used in high-power direct-to-chip liquid cooling in data centers.

Modern high-performance central processing units (CPU) and graphics processing units (GPU) feature high power densities and are continuously being miniaturized. Nonuniform heat distribution in multichip modules and modern multicore processing units has increased package reliability as well as exacerbated thermal management concerns. Typical thermal design power (TDP) today on modern CPUs and GPUs is approaching the mark of 400 W and will soon exceed this limit.^{1,2} It is evident from this that a

large amount of the heat dissipated in a typical data center server is attributed to the CPUs or GPUs and the remainder of it by auxiliary components such as solid-state drives (SSDs), power supply units (PSUs), and network interface controller (NIC) cards.³ As power densities continue to increase, many data center owners and chip manufacturers recognize that air cooling may not be sufficient and are instead turning to more efficient liquid cooling technologies such as direct-to-chip and indirect-to-chip liquid cooling technology.

Lochan Sai Reddy Chinthaparthy is a Ph.D. student, Himanshu Girishchandra Modi is a Ph.D. student and Dereje Agonafer, Ph.D., is a professor at the University of Texas at Arlington. Satyam Saini, Ph.D., is a thermal engineer at Intel Corporation. Pardeep Shahi, Ph.D., is a senior mechanical engineer at Nvidia Corporation. Pratik Vithoba Bansode, Ph.D., is a thermal engineer at Liquid Stack Corporation.

Reprinting of this proof for distribution or posting on web sites is not permitted. Authors may request from the editor an electronic file of the published article to reprint or post on their website once the final version has been published.

Direct-to-chip liquid-cooled servers consist of multiple cold plates connected to manifold networks. These manifolds contain dissimilar materials based on expected thermal and flow conditions, making it difficult to predict failure modes and their mechanisms. Metallic corrosion and erosion-corrosion are dominant failure modes in closed-loop cooling circuits, and detecting the source can be challenging. While the thermal and hydraulic performance of liquid-cooled servers is widely discussed in the literature, a lack of information exists on the reliability aspects of direct-to-chip liquid cooling.

ASHRAE guidelines recommend wetted materials for liquid-cooled data centers. While the guidelines provide a risk-based corrosion mitigation strategy, the corrosion process may vary due to flow and thermal conditions. ⁴ The pH level of the coolant may also affect cold plate corrosion, reducing cooling system reliability. As the temperature increases, pH levels vary, affecting corrosion rates.

Mohapatra reviewed various dielectric fluids suitable for direct-to-chip liquid cooling and listed deionized water, calcium chloride solution, propylene glycol and ethylene glycol as potential coolants.⁵ Propylene glycol is commonly used for secondary cooling loops in data centers due to its lower risk of corrosivity with varying percentages of ethylene glycol. Properly inhibited propylene glycol above 25% can help prevent bio growth and offer freezing protection for IT equipment in colder climates. However, it has lower thermal conductivity and higher pumping power requirements due to its higher viscosity in comparison with deionized water. Adding methanol and ethanol to the fluids increases flammability, and methanol is highly toxic. Potassium acetate and calcium chloride can be added to reduce the freezing point of the fluid. Fluorinated compounds like hydrofluoroethers (HFE) and FC-77 are popular for electronic component cooling but are more expensive and have lower thermal conductivity and specific heat than water-based fluids. 6,7

Corrosion occurs when the copper reacts with the surrounding coolant. Propylene and ethylene glycols at elevated temperatures accelerate corrosion on the copper surface. Corrosion affects data center performance and causes pitting and galvanic corrosion on the cold plate (*Online Figure 1* and *Online Figure 2*). (Visit https://tinyurl.com/JournalExtras for these and

other Online Figures.) Pitting creates cavities, and galvanic corrosion occurs when dissimilar metals are exposed to a conducting medium. Previous studies compared corrosion rates of cold plates under different conditions. A kinematic model was designed to predict the materials' reliability. 9

Effect of Corrosion

Corrosion can affect the functioning of a liquid cooling system in multiple ways. When copper corrodes and copper oxide and copper hydroxide are formed, as shown in the equations below, copper oxide formation in the microchannel fin area creates pores, which can disrupt the flow and require higher pumping power.

$$Cu^{0} + H_{2}^{1}O \rightarrow Cu^{2}O + H_{2}^{0}$$
 (1)

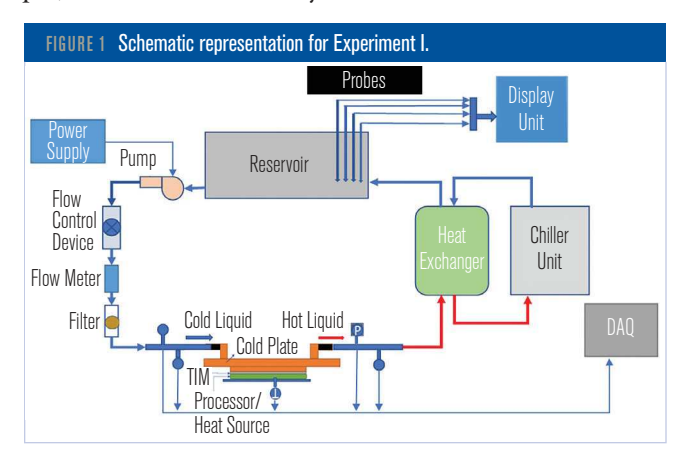
$$Cu^{2} + 2H_{2}O \rightarrow Cu(OH)_{2} + 2H^{+}$$
 (2)

Oxide deposition can cause blockages and leaks, reducing reliability and increasing repair costs.

Corrosion can be detected by monitoring pH, conductivity and oxidation-reduction potential. This article discusses two experiments: accelerated corrosion using inhibited liquids (Experiment 1) and elevated temperature effects on liquid properties with and without wetted materials (Experiment II).

Experiment IMethodology

The experiment employs coolants frequently used in operational data centers—all have been prediluted with corrosion inhibitors. The setup includes a reservoir that houses probes/electrodes submerged in the liquid for pH, electrical conductivity and oxidation-reduction



TECHNICAL FEATURE

potential. The fluid flows through a heat exchanger, maintaining the reservoir at an elevated temperature. The experimental schematic is shown in *Figure 1*.

Setup

The closed-loop setup consists of a copper microchannel cold plate mounted on a 1,000 watt ceramic heater with thermal interface material (TIM) in between. Inhibited coolants (*Table 1*) are circulated in the loop and via the heat exchanger by the centrifugal pump. A micro-mesh filter is fitted to remove particulate contaminants if any, and a flow control device is equipped to regulate the coolant flow rate. Thermistors and pressure sensors that have been calibrated were affixed at the cold plate's inlet and outlet. In the reservoir, calibrated pH and conductivity sensors were immersed. The data was logged using the appropriate data acquisition unit. The experimental setup is shown in *Figure 2*.

Procedure

For the initial experiment, a mixture of deionized (DI) water and industrial antimicrobial agent solution is run through the loop to eliminate any existing salts or bacterial growth. After draining the solution and rinsing it with DI water, the coolant is added to the reservoir. The pump is then turned on and adjusted to achieve a flow rate of 0.5 L/min (0.02 cfm), and any bubbles in the loop are eliminated. The heater is then powered on and set to 350 watts, and the heat exchanger is connected

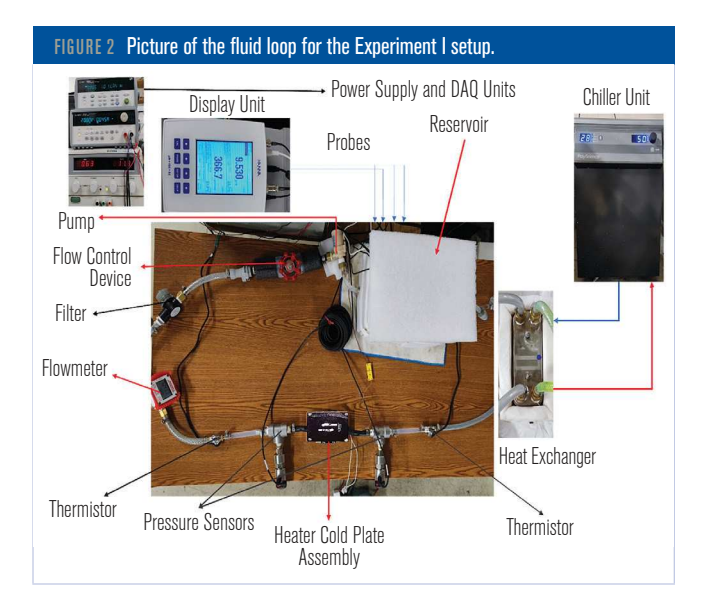


TABLE 1 Properties of all liquids used in the experiment.						
	COLOR	DENSITY	VISCOSITY	FREEZING Point	BOILING POINT	THERMAL CONDUCTIVITY
PG-25	Colorless	1.021 g/cm ³	2.45 mPa·s	-10.1°C	101°C	0.4625 W/m·K
PG-55	Colorless	1.042 g/cm ³	6.19 mPa·s	-43.3°C	106.1°C	0.324 W/m·K
EG-25	Colorless	1.040 g/cm ³	2.09 mPa·s	-12.6°C	103.1°C	0.494 W/m·K
EG-55	Colorless	1.088 g/cm ³	5.77 mPa·s	-45.3°C	107.9°C	0.377 W/m·K

to a chiller set to provide a coolant inlet temperature of 50°C (122°F). Temperature and pressure readings, along with pH, conductivity and oxidation reduction potential (ORP) values, are logged once the system has reached a steady state.

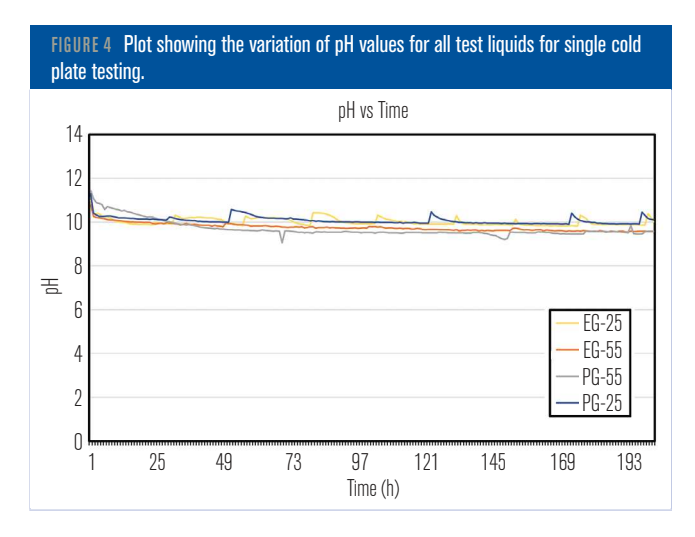


The second experiment uses four coolants—two polyethylene glycol and two ethylene glycol; PG-25, PG-55, EG-25 and EG-55 stored in airtight jars at elevated temperatures (*Figure 3*). Two variations were studied: one with periodic exposure to outside air every 12 hours and the other with no outside air exposure. Both had two sets of jars, Set I containing only the sample liquids and Set II including wetted materials such as EPDM rubber hoses, brass, steel and copper. The experiment compares the effects of the coolants' properties when in a closed container and when stagnating in a closed loop of an unused server.

Procedure

The jars were cleansed with DI water, and the coolants were added once the jars dried. We set the program for the chamber to run at 70°C (158°F). After noting the initial readings of pH, conductivity and ORP, the jars are closed and kept in the chamber, and the program is executed. In the experiment's first variation, the liquids are exposed to outside air before the readings are taken for both sets twice every 24 hours. For the second variation, initial and final readings are noted as liquids





will be exposed if the jars were opened for readings.

Results and Discussion

Experiment I

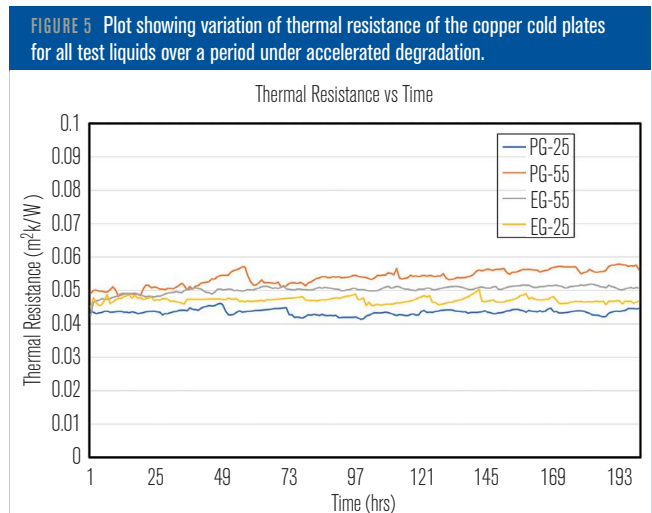
Four glycol liquids (PG-55, PG-25, EG-25 and EG-55) underwent an experimental procedure in which probes that were inserted in the reservoir monitored their chemistry changes.

During the experiment, elevated temperature conditions caused water molecules in the liquids to break down into hydrogen and oxygen atoms, causing an increase in pH levels. From *Figure 4* the highest pH variation of 13.49% was observed in PG-55, and the least change of 4.64% was observed in PG-25. EG-25 had a 5.33% reduction, and EG-55 had a 6.72% reduction in pH value, indicating that all liquids were less basic than their initial states.

PG-55 had the highest conductivity variation of 34.56%, while PG-25 had the least change of 2.87%. EG-25 and EG-55 had 3.71% and 3.18% less conductivity than their initial values, respectively (*Online Figure 3*). *Online Figure 4* shows reduced charge carriers from their initial states.

All liquids had high ORP values, which could cause corrosion of copper cold plates. From *Online Figure 4* the highest ORP change of 87.8 mV was observed in PG-55, and the least change of 29.4 mV was observed in EG-25. PG-25 and EG-55 had ORP differences of 50.1 mV and 65.8 mV, respectively, from their initial values.

The thermal resistance of the cold plate for all four fluids was measured by logging inlet and base temperatures. Corrosion formation caused thermal resistance variation by reducing thermal conductivity.



From *Figure 5*, PG-25 showed a 1.36% increase, the least, while EG-55 had the highest change at 19.29%. PG-55 increased to 14.48%, and EG-25 changed by 3.32% from initial thermal resistance.

Pressure difference indicates microchannel corrosion. Copper oxides or pits can disrupt flow and increase pressure drop. From *Figure 6* we can state that PG-25 had the lowest change at 7.72%, and PG-55 had the highest at 37.31%. EG-25 had a 24.66% increase, while EG-55 had a 9.19% increase in pressure drop.

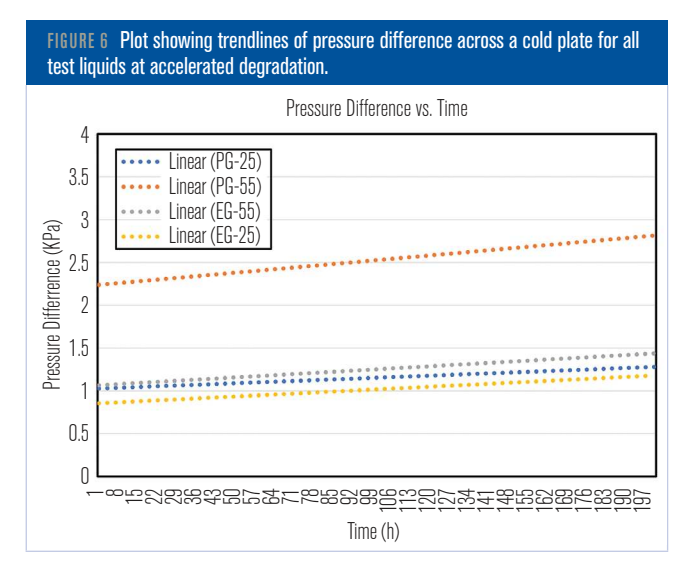
Experiment II

Variation I

The second experiment involved airtight jars placed in an environmental chamber to maintain elevated temperatures. Set I observed coolant chemistry under stagnated conditions, while Set II had a combination of commonly used wetted materials. Both were briefly exposed to surrounding air, representing typical maintenance scenarios. Results from Set I are as follows.

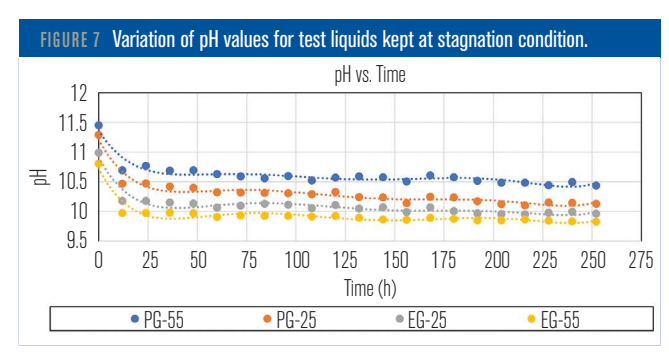
Figure 7 and Online Figure 5 show the change in pH values for plain test liquids and test liquids with wetted material immersed, respectively. EG-55 had the least change in pH value, decreasing by 1.4% with no wetted materials immersed, but had the highest reduction of 14.4% when parts were immersed. EG-25 had a 2.1% reduction in Set I and a 3.2% reduction in Set II. PG-55 had a 2.4% reduction in Set I and a 3.4% reduction in Set II, while PG-25 had a 3.2% reduction in Set I, and a 4.2% reduction in Set II.

Online Figures 6 and 7 show changes in conductivity values for plain and wetted materials immersed in test



liquids, respectively. PG-25 had the least reduction of 4.2% and 3.8% in both sets, while PG-55 had the highest reduction of 54.8% and 13.5%. EG-25 showed a reduction of 12.47% and 2.7%, while EG-55 had reductions of 12.9% and 8.2% in Set I and Set II, respectively.

ORP values indicate a liquid's potential to oxidize



metal surfaces; higher ORP values indicate increased oxidation reactions. *Online Figure 8* shows ORP changes for Set I test liquids (those under stagnated conditions), and *Online Figure 9* shows ORP changes for Set II liquids with immersed wetted materials. PG-55 had the least ORP increase, while PG-25 had the highest. EG-55 and EG-25 had 50 mV to 51 mV increases. In the presence of materials, PG-25 had the highest ORP increase (1 7 N), and EG-25 had ORP increases of 93.8 mV and 83 mV, respectively.

Variation II

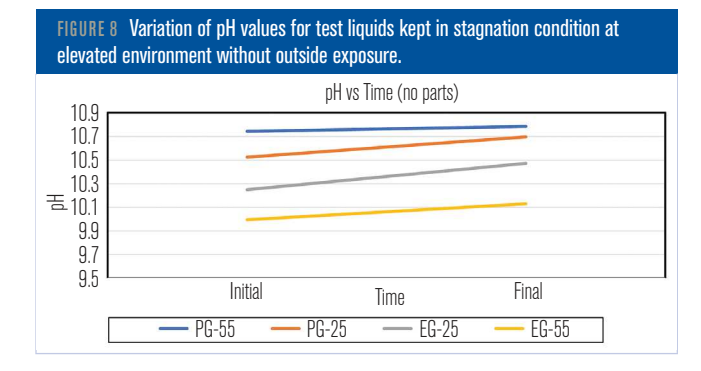
In this set of experiments, the liquids were kept inside an airtight jar for the same amount of time as in Set I, and only the initial and final readings were measured to avoid exposure of the liquid to the surrounding atmosphere. This can give us the comparison of liquid chemistry that was never in contact with air and that was exposed to the outside air.

In stagnated conditions, liquids concealed from outside air have better noncorrosive properties. In Set I, the pH values of liquids increased by their base value when compared to those immersed in wetted materials. Without wetted materials, EG-25 and PG-25 showed 2.17% and 1.62% increases in pH value, respectively. PG-55 had the least increase of 0.39%, and EG-55 had a 1.35% increase in pH value (*Figure 8*).

Online Figure 10 shows the pH values for wetted materials immersed. Only EG-25 had an increase in pH value, of 0.087%. The other liquids had a decrease, with EG-55 showing the highest decrease at 2.57%, followed by PG-55 at 2.07% and PG-25 at 0.77%.

Online Figure 11 shows that for Set I, the highest change was in EG-55 with a 2.62% increase in conductivity value and PG-55 with a 2.23% increase in conductivity value. The other two liquids, EG-25 and PG-25, had the same

TECHNICAL FEATURE



conductivity value at the end of the experiment.

Online Figure 12 shows that for Set II, only EG-25 had a 4.5% increase in conductivity value. EG-55, PG-55 and PG-25 had a decrease in conductivity level ranging from 1.5% to 2.7% from their initial values.

Online Figure 13 shows that Set I had a lower ORP value, indicating reduced corrosive properties. The highest decrease was in PG-25, and the least change was in EG-25. In Online Figure 14, Set II with wetted materials had reduced ORP values except for PG-55, which had an increase. EG-25 had the highest reduction of 50 mV,

EG-55 had 7.6 mV less and PG-25 had a value like the beginning.

Conclusion

During accelerated degradation at the cold plate level, test liquids showed decreased chemical properties. PG-25 had the least change of 4.6% in pH, 2.8% in conductivity and EG-25 had the least change in ORP. PG-25 had the least effect on metal surface corrosiveness, thermal resistance and pressure drop.

In the second experiment, liquids showed advantages in different areas. EG-55 had a 1.4% pH reduction in the no-parts immersed case, while EG-25 had the least reduction of 3.2% in the presence of wetted materials. PG-25 had the least reduction in conductivity without wetted materials, and EG-25 had a 2.7% reduction in their presence. PG-55 had the least increase in ORP value without wetted materials, and EG-25 had the least increase in the immersed case.

Liquid characteristics significantly changed in jars with no outside air exposure. PG-55 had a 0.39%

TECHNICAL FEATURE

decrease, and PG-25 had a 1.62% decrease in the pH value. EG-55 had an increase in pH, and PG-25 had the least decrease of 0.77%. The conductivity of EG-55 and PG-55 increased, and EG-25 had a 4.5% increase when parts were present. PG-25 had the highest decrease in ORP when wetted materials were absent, and EG-25 had the highest decrease in ORP value in the other plot.

Future Work

The procedure was performed at elevated temperatures to accelerate material performance degradation. Multiple cold plates will undergo long test runs (up to 90 days) to observe changes in fluid chemistry and cold plate performance. Scanning electron microscopy will identify foreign materials on the microchannel surfaces, and Fourier transforminfrared spectroscopy will detect copper or corroded substrate presence. Propylene glycols are preferred over ethylene glycols due to their antibacterial growth property, and the initial and concluding bacterial

growth for each liquid will be compared by direct and indirect methods like turbidimetry.

References

- 1. Intel. Undated. "Intel® Xeon® Platinum 9282 Processor." Intel.
- 2. NVIDIA. 2021. "NVIDIA A100 Tensor Core GPU." NVIDIA.
- 3. Day, T., P. Lin, R. Bunger. 2019, "Liquid Cooling Technologies for Data Centers and Edge Applications." Schneider Electric-Data Center Science Center, White Paper No. 265.
- 4. ASHRAE. 2013. Liquid Cooling Guidelines for Datacom Equipment Centers, Second Ed. Peachtree Corners, GA: ASHRAE.
- 5. Mohapatra, S. 2006. "An overview of liquid coolants for electronics cooling." $\it Electronics Cooling$ (2).
- 6. Aittomäki, A., A. Lahti. 1997. "Potassium formate as a secondary refrigerant." *International Journal of Refrigeration* 20(4):276–282.
- 7. Chrysler, G.M., R.C. Chu, R.E. Simons. 1994. "Jet impingement boiling of a dielectric coolant in narrow gaps." *Proceedings of 1994 4th Intersociety Conference on Thermal Phenomena in Electronic Systems* 1–8.
- 8. Kini, G., et al. 2020. "Corrosion in liquid cooling systems with water-based coolant—part 1: flow loop design for reliability tests." 2020 19th IEEE Intersociety Conference on Thermal and Thermomechanical Phenomena in Electronic Systems (ITherm) 422–428.
- 9. Kim, C.U., et al. 2020. "Corrosion in liquid cooling systems with water-based coolant—part 2: corrosion reliability testing and failure model." 2020 19th IEEE Intersociety Conference on Thermal and Thermomechanical Phenomena in Electronic Systems (ITherm) 429–434

Reprinting of this proof for distribution or posting on web sites is not permitted. Authors may request from the editor an electronic file of the published article to reprint or post on their website once the final version has been published.

